Available online at www.sciencedirect.com
ScienceDirect
ELSEVIER
Systems & Control Letters ■■■ (■■■■) ■■■–■■■
SYSTEMS & CONTROL LETTERS
www.elsevier.com/locate/sysconle

Coordinated patterns of unit speed particles on a closed curve

Fumin Zhang, Naomi Ehrich Leonard*

Department of Mechanical and Aerospace Engineering, Princeton University, Princeton, NJ 08544, USA

Received 15 June 2006; received in revised form 28 September 2006; accepted 31 October 2006

Abstract

We present methods to stabilize a class of motion patterns for unit speed particles in the plane. From their initial positions within a compact set in the plane, all particles converge to travel along a closed curve. The relative distance between each pair of particles along the curve is measured using the relative arc-length between the particles. These distances are controlled to converge to constant values.

Keywords: Pattern; Formation; Swarm; Cooperative control; Gyroscopic control; Tracking; Oscillator

1. Introduction

Agile sensor networks can collect information in the sky, on the ground and underwater. Sensor networks with fixed nodes are able to continuously monitor specific locations for long periods of time. Great research progress has been achieved and commercial products are emerging cf. [6].

A new direction for sensor network research employs satellites, unmanned aerial vehicles (UAVs), ground robots and unmanned underwater vehicles (UUVs) as moving sensor platforms. Such a mobile sensor network can cover a large area with a relatively small number of platforms by performing cooperative motion that ensures the optimal distribution of sensing power across the area. Some of the latest research results demonstrate that control over relative positions among sensor platforms has significant impact on the quality of information collected by the entire network cf. [15,16,20,35].

Influenced by the study of swarming behaviors of animal groups cf. [22], researchers are developing cooperative control methods to achieve the desired relative positions among a group of moving sensor platforms. The problem is often called the swarming or formation problem. The dynamics of each platform in the network is usually complicated. For coordination purposes, however, it is practical to use the simpler model of an individual platform modeled as a particle in the sense of classical mechanics. One advantage of using this simple model is that the theoretical results are platform independent. Error caused by this simplification is usually reduced by a lower level, platform specific controlling mechanism. This is true, for example, in the case of a recent experimental demonstration of controlling a fleet of underwater gliders [30]. The particles interact with each other through synthetic forces that are induced by feedback control laws. The goal is to devise suitable control laws so that the particles attain desired motion patterns. In this spirit, methods such as energy shaping [4,27] are applied with promising results for formations in the plane cf. [19,31]. The literature is also rich with results regarding cooperative control where particles are replaced by agents with simple dynamics, for example in [2,8,21].

Operational objectives for UAVs and UUVs often require the platforms to travel at the highest constant speed to survey the largest area in unit time. Therefore, one may also view the platforms as particles moving at (common) constant speed. Particles under gyroscopic forces obey a constant speed constraint. Certain patterns for a system of particles with unit speed can be classified. Using Lie group theoretic methods, Justh and Krishnaprasad have shown that in the plane, particles moving along parallel lines or around the same circle are the only relative equilibria if the particles are subjected to steering laws that depend only on relative positions and headings. Steering control laws are proposed to asymptotically achieve those patterns as

* Corresponding author.
E-mail address: naomi@princeton.edu (N.E. Leonard).

0167-6911/$ - see front matter © 2006 Published by Elsevier B.V.
doi:10.1016/j.sysconle.2006.10.027

Please cite this article as: F. Zhang, N.E. Leonard, Coordinated patterns of unit speed particles on a closed curve, Systems Control Lett. (2006), doi: 10.1016/j.sysconle.2006.10.027

relative equilibria cf. [11] and an earlier version [9]. The insight also enabled the work in [29,32] to design (time varying) steering control for obstacle avoidance and boundary following for a single constant speed particle.

The steering control laws given in [11] are justified for achieving planar formations of two unit speed particles. Extension to many particles are made in [10]. Sepulchre et al. [24] noticed that patterns of many constant speed particles can be achieved in the plane by extending methods previously developed for coupled oscillators [25]. In [24], steering control laws are developed to stabilize formations on circles and parallel lines. It is later shown in [15] that ellipses can be mapped to circles using a nonlinear transform so that some of the results in [24] can be generalized to ellipses.

In applications such as the Adaptive Sampling and Prediction of the ocean (ASAP) project [1], desired coordinated trajectories for mobile sensor platforms are defined by a collection of closed curves of various shape with prescribed relative spacing of vehicles on the curves. These are computed both to minimize sensing error and to address operational challenges. This has motivated the need for a systematic method to design steering control laws that stabilize patterns on a closed curve with arbitrary shape. In this paper, we first modify methods in [29,32] to steer one agent so that its trajectory converges to the desired closed curve. Next, to achieve a prescribed collective motion pattern, we address the major challenge of the inhomogeneity of phase angles of particles around the closed curve. Influenced by the ideas in [33,34], we propose a method that uses the relative arc-length between particles instead of phase angle differences to measure the relative position between agents on a closed curve. Our steering control laws are proved stable using a Lyapunov function that converges to its critical point along the controlled dynamics.

The paper is organized as follows. In Section 2, we define an orbit function on the plane. The level sets of this orbit function can be viewed as orbits with energy equal to the function value. In Section 3, we develop the equations describing the motion of a unit speed particle with respect to the orbits. In Section 4, a control law for two particles is developed to stabilize patterns on any given orbit. The coupling between the two particles is a function of the relative curve length. We generalize the control law to a collection of N particles in Section 5. We demonstrate the control laws with simulation results presented in Section 6.

2. Orbit function

Let $\gamma_0(\cdot)$ represent a simple, closed, regular curve in the plane parametrized by its arc-length s. The total length L of such a curve is finite. A point $\vec{q}_0$ on the curve is selected as the *starting point* and at this point we assign $s=0$. The Frenet–Serret frame $(\vec{x}_0(s), \vec{y}_0(s))$ can be constructed with $\vec{x}_0(s)$ the unit tangent vector to the curve and $\vec{y}_0(s)$ the unit normal vector to the curve at $\gamma_0(s)$. We use the convention such that $(\vec{x}_0(s), \vec{y}_0(s))$ forms a right-handed coordinate frame with $\vec{x}_0(s) \times \vec{y}_0(s)$ pointing to the reader. Let $\kappa(s)$ be the curvature of the curve at $\gamma_0(s)$. The Frenet–Serret equations describe how the frame formed by $(\vec{x}_0(s), \vec{y}_0(s))$ is translated along the curve:

$$\frac{\mathrm{d}\vec{x}_0(s)}{\mathrm{d}s} = \kappa(s)\vec{y}_0(s),$$
$$\frac{\mathrm{d}\vec{y}_0(s)}{\mathrm{d}s} = -\kappa(s)\vec{x}_0(s). \tag{1}$$

Without loss of generality, we assume that the origin of a lab fixed coordinate system is placed at a point in the plane encircled by $\gamma_0(\cdot)$. Notice that since the curve is a compact subset of the plane, we can construct a closed ball B centered at the origin such that $\gamma_0(\cdot) \in \mathrm{int}(B)$.

Lemma 1. *Assume that at every point on the curve γ_0, the curvature is uniformly bounded. There exists a function $z : B \to \mathbb{R}$, satisfying the following properties*:

(A1) *γ_0 is a level curve of $z(\cdot)$ i.e., $z(\gamma_0(\cdot))$ is a constant function of s.*
(A2) *There exists a finite interval $[c_1, c_2]$ such that any level curve of $z(\cdot)$ with its value belonging to $[c_1, c_2]$ is entirely contained in B. Also, $z(\gamma_0(\cdot)) \in (c_1, c_2)$.*
(A3) *The function z is smooth on the open set $\Omega = \{\vec{r} \in B | c_1 < z(\vec{r}) < c_2\}$. Furthermore, $\|\nabla z\| \neq 0$ for all points in Ω.*

Proof. Near $\gamma_0(\cdot)$, a family of curves $\gamma_\lambda(\cdot)$, called the Bertrand family cf. [18], can be constructed as $\gamma_\lambda(s) = \gamma_0(s) + \lambda\vec{y}_0(s)$ where λ is a real number. The tangent vector to $\gamma_\lambda(s)$ is $\vec{x}_\lambda(s) = (1 - \kappa(s)\lambda)\vec{x}_0(s)$. There is a singularity at $\lambda = 1/\kappa$. Because we assume that $\kappa(s)$ is uniformly bounded for all s, we may choose an $\varepsilon \in (0, 1/\sup\{|\kappa(s)|\})$ so that all Bertrand curves with $|\lambda| \leqslant \varepsilon$ are regular and are contained in B. We let the set Ω be defined as the set of all points on the Bertrand curves with $|\lambda| < \varepsilon$. It can be verified that Ω is an open connected subset of B.

Since every point in Ω belongs to a Bertrand curve, we can construct a function $z(\vec{r})$ on Ω by letting $z(\vec{r}) = \lambda$ if $\vec{r} \in \gamma_\lambda(\cdot)$. Each Bertrand curve is a level curve for $z(\vec{r})$. We now select an arbitrary point $\vec{r}$ and prove that $z(\vec{r})$ is differentiable at $\vec{r}$. In fact, within a small neighborhood of $\vec{r}$, the directional derivative of $z(\vec{r})$ along the tangent vector $\vec{x}_\lambda(s)$ is always 0. The directional derivative of $z(\vec{r})$ along the normal vector $\vec{y}_\lambda(s)$ is always constantly 1 or -1. The sign depends on whether λ is increasing or decreasing along the $\vec{y}_\lambda$ direction. The continuity of these two directional derivatives implies that $z(\vec{r})$ is differentiable in the selected neighborhood.It is a property of the Bertrand family of curves that $\vec{y}_\lambda(s) = \vec{y}_0(s)$. Therefore, since $\nabla z = \vec{y}_0(s)$ or $\nabla z = -\vec{y}_0(s)$, ∇z is a smooth vector field. Thus $z(\vec{r})$ is smooth in the neighborhood. Since these arguments hold for all points in Ω, $z(\vec{r})$ is smooth in Ω. Notice also that $\|\nabla z\| = 1 \neq 0$ for all points in Ω.

We may let $z(\vec{r}) = 0$ for $\vec{r} \in B/\Omega$ and let $c_1 = -\varepsilon$ and $c_2 = +\varepsilon$. This concludes the proof since we have given one method to construct a function z that satisfies all properties in the lemma. □

Please cite this article as: F. Zhang, N.E. Leonard, Coordinated patterns of unit speed particles on a closed curve, Systems Control Lett. (2006), doi: 10.1016/j.sysconle.2006.10.027

We emphasize that the method given in the proof is often not the best for constructing the function $z(\cdot)$. Simple methods for special curves often result in a much larger Ω. For example, suppose an ellipse is given by $\vec{r} = (x, y) \in \mathbb{R}^2$ and $x^2/a^2 + y^2/b^2 = 1$ for constants $a, b \in \mathbb{R}$. We may define a function $z(\vec{r}) = x^2/a^2 + y^2/b^2$. The level curves of $z(\cdot)$ are families of concentric ellipses. We can choose c_1 to be an arbitrarily small positive number and $c_2 > c_1$ to be an arbitrarily large positive number. The set $\Omega = \{\vec{r} \in \mathbb{R}^2 | c_1 < z(\vec{r}) < c_2\}$ is an arbitrarily large bounded set without the origin.

In the above example, if we let the starting point of each ellipse be the intersection of the ellipse with the horizontal axis, then all starting points are on a smooth curve which is a straight line. In general, we have the following result.

Lemma 2. *A starting point for each level curve of z in the set Ω can be selected such that the starting points form a smooth curve.*

Proof. We can write down a differential equation describing the gradient flow of $z(\vec{r})$ that generates trajectories with their tangent vectors identical to the gradient vectors

$$\frac{\mathrm{d}\vec{q}}{\mathrm{d}\tau} = \nabla z(\vec{q}(\tau)). \tag{2}$$

Starting from the point $\vec{q}_0$ which is the starting point for $\gamma_0(\cdot)$, the solution of this equation $\vec{q}(\tau)$ produces a smooth curve. Because ∇z is smooth on Ω, the solution of this differential equation exists and is unique for τ increasing or decreasing. Furthermore, the solution curve intersects all level curves in Ω. We may choose one intersection point for each curve to be the starting point. □

We call the function $z(\cdot)$ which satisfies the properties in Lemma 1 the *orbit function*. Each level curve of this orbit function is called an *orbit*. We call the selected curve $\gamma_0(\cdot)$ the *reference orbit*. A point $\vec{r}$ in the set Ω is uniquely determined by knowing $z(\vec{r})$ which we call the *orbit value* and $s(\vec{r})$ which is the arc-length measured from the starting point of the orbit with value $z(\vec{r})$. These definitions are illustrated in Fig. 1.

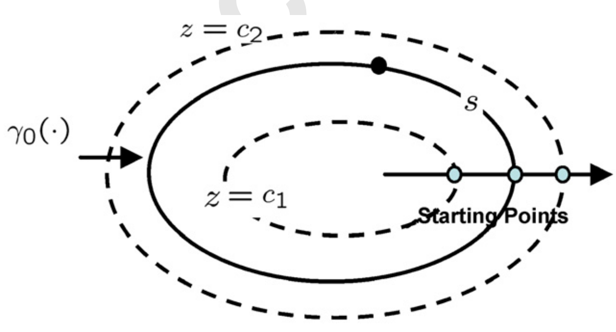

Fig. 1. A set of concentric ellipses. The inner ellipse has orbit value c_1 and outer ellipse has orbit value c_2. The curve length s is measured from the starting point of $\gamma_0(\cdot)$ (solid ellipse) to the position of the particle (black circle) on $\gamma_0(\cdot)$.

Note that we do not require the orbits to belong to a Bertrand family, even though we can construct a set of orbits that belong to a Bertrand family for a single-looped regular curve with arbitrary shape using the methods in the proof of Lemma 1.

3. Orbit of unit speed particle

Let $\vec{r}$ be the position of a unit speed particle. Suppose $\vec{r} \in \Omega$ at time t, then $\vec{r}$ belongs to an orbit $\gamma(\cdot)$ with orbit value $z(\vec{r})$. The tangent vector to the curve at $\gamma(s)$ is not necessarily aligned with the velocity vector of the particle at $\vec{r}$. Let the Frenet–Serret frame along orbit $\gamma(\cdot)$ be $(\vec{x}_1, \vec{y}_1)$. Let the velocity vector of the particle be $\vec{x}$. We can establish another Frenet–Serret frame for the actual trajectory of the particle by selecting a normal vector $\vec{y}$ perpendicular to $\vec{x}$ that forms a right-handed coordinate frame with $\vec{y}$ so that $\vec{x} \times \vec{y}$ points to the reader, as shown in Fig. 2. Our goal is to develop the differential equations that describe the change of the two frames and their relative displacement as the particle moves.

The motion of the frame formed by $(\vec{x}, \vec{y})$ of the unit speed particle is

$$\dot{\vec{x}} = u_1 \vec{y},$$
$$\dot{\vec{y}} = -u_1 \vec{x}, \tag{3}$$

where u_1 is the steering control of the vehicle. We define an angle $\theta_1 \in (-\pi, \pi]$ as

$$\cos\theta_1 = \vec{x} \cdot \vec{x}_1 = \vec{y} \cdot \vec{y}_1,$$
$$\sin\theta_1 = \vec{y} \cdot \vec{x}_1 = -\vec{x} \cdot \vec{y}_1. \tag{4}$$

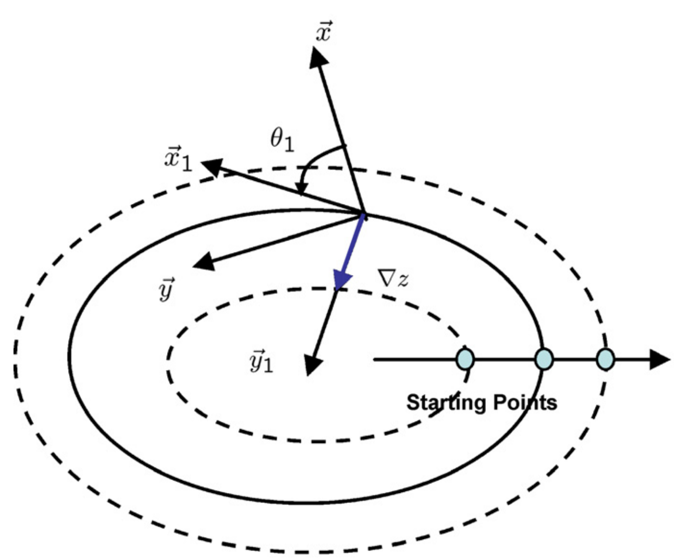

Fig. 2. The two Frenet–Serret frames established at the position of a unit speed particle $\vec{r}$. $\vec{x}_1$ is tangent to the closed level curve of function $z(\cdot)$. $\vec{x}$ is the velocity vector of the particle. The angle θ_1 is also shown. In this case, the gradient vector $\nabla z(\vec{r})$ and $\vec{y}_1$ point in the same direction.

Please cite this article as: F. Zhang, N.E. Leonard, Coordinated patterns of unit speed particles on a closed curve, Systems Control Lett. (2006), doi: 10.1016/j.sysconle.2006.10.027

As the particle moves, the orbit value z of the particle changes as a function of time:

$$\frac{\mathrm{d}z}{\mathrm{d}t} = \nabla z \cdot \frac{\mathrm{d}\vec{r}}{\mathrm{d}t} = \nabla z \cdot \vec{x} = \pm \|\nabla z\| \vec{y}_1 \cdot \vec{x} \\ = \mp \|\nabla z\| \sin\theta_1. \tag{5}$$

The sign depends on whether ∇z is aligned with $\vec{y}_1$ or points in the opposite direction of $\vec{y}_1$. The plus sign in the final expression of (5) is assumed when $\vec{y}_1 = -\nabla z/\|\nabla z\|$ and the minus sign is assumed when $\vec{y}_1 = \nabla z/\|\nabla z\|$. Notice that once the sign is determined, because the level curves are all closed curves and never intersect one another, the sign is fixed for all points in Ω. In this paper, for simplicity, we adopt the convention that $\vec{y}_1 = \nabla z/\|\nabla z\|$ so that only the minus sign is assumed in (5).

The frame $(\vec{x}_1, \vec{y}_1)$ changes as the particle moves. We first compute how $\vec{y}_1$ evolves:

$$\dot{\vec{y}}_1 = \frac{\nabla^2 z \dot{\vec{r}}}{\|\nabla z\|} - \frac{(\nabla z \cdot \nabla^2 z \dot{\vec{r}})\nabla z}{\|\nabla z\|^3} \\ = \frac{1}{\|\nabla z\|}(\nabla^2 z\vec{x} - (\vec{y}_1 \cdot \nabla^2 z\vec{x})\vec{y}_1), \tag{6}$$

where $\nabla^2 z$ is the Hessian matrix of function $z(\cdot)$ at point $\vec{r}$. Taking derivatives with respect to time on both sides of the second equation in (4) we have

$$\begin{aligned}\cos\theta_1 \dot{\theta}_1 &= -\dot{\vec{x}} \cdot \vec{y}_1 - \vec{x} \cdot \dot{\vec{y}}_1 \\ &= -(u_1 \vec{y}) \cdot \vec{y}_1 - \vec{x} \cdot \dot{\vec{y}}_1 \\ &= -u_1 \cos\theta_1 - \frac{1}{\|\nabla z\|} \\ &\quad \times (\vec{x} \cdot \nabla^2 z\vec{x} + (\vec{y}_1 \cdot \nabla^2 z\vec{x})\sin\theta_1).\end{aligned} \tag{7}$$

Since $\vec{x} = \cos\theta_1 \vec{x}_1 - \sin\theta_1 \vec{y}_1$, we know that

$$\vec{x} \cdot \nabla^2 z\vec{x} + (\vec{y}_1 \cdot \nabla^2 z\vec{x})\sin\theta_1 \\ = \cos^2\theta_1(\vec{x}_1 \cdot \nabla^2 z\vec{x}_1) - \sin\theta_1 \cos\theta_1(\vec{x}_1 \cdot \nabla^2 z\vec{y}_1). \tag{8}$$

Therefore,

$$\dot{\theta}_1 = \kappa_{\mathrm{a}} \cos\theta_1 + \kappa_{\mathrm{b}} \sin\theta_1 - u_1, \tag{9}$$

where we define

$$\kappa_a = -\frac{1}{\|\nabla z\|}\vec{x}_1 \cdot \nabla^2 z\vec{x}_1, \\ \kappa_b = \frac{1}{\|\nabla z\|}\vec{x}_1 \cdot \nabla^2 z\vec{y}_1. \tag{10}$$

We observe that the motion of the particle projected to $\vec{x}_1$ causes the arc-length s to change along the orbit. On the other hand, the motion of the particle projected to $\vec{y}_1$ causes orbit change which also induces variation in the arc-length s. Therefore, to compute the total variation of the arc-length, we reparametrize all curves using the arc-length parameter σ of the reference orbit $\gamma_0(\cdot)$. Then the arc-length s between the point $\vec{r} \in \Omega$ and the starting point of the orbit where $\vec{r}$ belongs is a function $s(z, \sigma)$. Furthermore, we can write,

$$s(z, \sigma) = \int_0^\sigma \frac{\partial s(z, \tau)}{\partial \tau}\,\mathrm{d}\tau. \tag{11}$$

Then, the total variation of arc-length is

$$\frac{\mathrm{d}s}{\mathrm{d}t} = \frac{\partial s(z,\sigma)}{\partial \sigma}\frac{\mathrm{d}\sigma}{\mathrm{d}t} + \frac{\partial s(z,\sigma)}{\partial z}\frac{\mathrm{d}z}{\mathrm{d}t} \\ = \left.\frac{\mathrm{d}s}{\mathrm{d}t}\right|_{z=\mathrm{const}} + \frac{\partial s(z,\sigma)}{\partial z}\frac{\mathrm{d}z}{\mathrm{d}t}. \tag{12}$$

We have

$$\left.\frac{\mathrm{d}s}{\mathrm{d}t}\right|_{z=\mathrm{const}} = \frac{\mathrm{d}\vec{r}}{\mathrm{d}t} \cdot \vec{x}_1 = \vec{x} \cdot \vec{x}_1 = \cos\theta_1. \tag{13}$$

Therefore,

$$\frac{\mathrm{d}s}{\mathrm{d}t} = \cos\theta_1 + \frac{\partial s(z,\sigma)}{\partial z}\frac{\mathrm{d}z}{\mathrm{d}t} \\ = \cos\theta_1 - \frac{\partial s}{\partial z}(z,\sigma)\|\nabla z\|\sin\theta_1. \tag{14}$$

Since

$$\frac{\partial s(z,\sigma)}{\partial z} = \int_0^\sigma \frac{\partial^2 s(z,\tau)}{\partial z\,\partial \tau}\,\mathrm{d}\tau, \tag{15}$$

if $\partial^2 s(z,\tau)/\partial z \partial \tau$ is not constantly 0 along a simple closed curve, then $\partial s/\partial z$ is not a constant when a particle moves along that curve.

4. A two particle pattern

We now consider the case of controlling two unit speed particles to a common orbit with prescribed arc-length separation. Let $\gamma_1(\cdot)$ and $\gamma_2(\cdot)$ be the instantaneous orbits for particles 1 and 2, respectively. Let s_1 and s_2 be the curve lengths measured from the starting points of $\gamma_1(\cdot)$ and $\gamma_2(\cdot)$, respectively. Let z_1 and z_2 be the corresponding orbit values of the two instantaneous orbits. We want to design a controller that drives the system asymptotically to

$$z_1 = z_2 = c_z \quad \text{and} \quad s_1 - s_2 = c_s, \tag{16}$$

where $c_z \in (c_1, c_2)$ (see Lemma 1) and $c_s \in [0, L)$ where L is the total length of the orbit with orbit value c_z. We say c_z and c_s determine an *invariant pattern* for two unit speed particles defined by (16). Without loss of generality, we select orbit c_z as the reference orbit. Then our goal is to stabilize an invariant pattern for two unit speed particles on the reference orbit.

The total length of γ_1 and the total length of γ_2 are finite. To prevent s_1 and s_2 from getting arbitrarily large, we make use of two angle variables:

$$\psi_1 = \frac{2\pi}{L}(s_1 \bmod L) \quad \text{and} \quad \psi_2 = \frac{2\pi}{L}(s_2 \bmod L), \tag{17}$$

where $(s_1 \bmod L)$ and $(s_2 \bmod L)$ are bounded by L. The derivative of ψ_i with respect to time satisfies

$$\frac{\mathrm{d}\psi_i}{\mathrm{d}t} = \frac{2\pi}{L}\left(\cos\theta_i - \frac{\partial s_i}{\partial z_i}\|\nabla z_i\|\sin\theta_i\right), \tag{18}$$

where θ_i is the angle between the velocity vector and the tangent vector to the instantaneous orbit, as defined in (4) but for the ith particle.

Please cite this article as: F. Zhang, N.E. Leonard, Coordinated patterns of unit speed particles on a closed curve, Systems Control Lett. (2006), doi: 10.1016/j.sysconle.2006.10.027

Using the curve length parameter σ for the reference orbit, we have

$$(s_i \bmod L) = \frac{2\pi}{L} \int_{\sigma_{0i}}^{\sigma_i} \frac{\partial s(z_i, \tau)}{\partial \tau}\, \mathrm{d}\tau \tag{19}$$

for $i = 1, 2$, where σ_{0i} marks the latest point on the orbit where s_i changes from L to 0. Therefore in (18),

$$\frac{\partial s_i}{\partial z_i} = \int_{\sigma_{0i}}^{\sigma_i} \frac{\partial^2 s_i(z_i, \tau)}{\partial z_i\, \partial \tau}\, \mathrm{d}\tau. \tag{20}$$

As a function of σ_i, $\partial s_i/\partial z_i$ is not continuous when $(\sigma_i - \sigma_{0i}) \to L$. But it is straightforward to see that $\partial s_i/\partial z_i$ is piecewise continuous. The function $\partial s_i/\partial z_i$ is still smooth for the values of σ_i such that $\sigma_i \in (\sigma_{0i}, \sigma_{0i} + L)$. Later we will see that this discontinuity requires special treatment in the proof for convergence of our control laws.

In order to measure the relative arc-length difference, we define $\Phi = \psi_1 - \psi_2 - 2\pi c_s/L$ where $0 < c_s < L$ represents the desired arc-length separation between the two particles. Without loss of generality we study the case when $\Phi \in (-\pi, \pi)$. The state of the two particles are now determined by $(z_1, z_2, \theta_1, \theta_2, \Phi)$. We define the state space S to be the set of all the states satisfying $z_1 \in (c_1, c_2)$, $z_2 \in (c_1, c_2)$, $\theta_1 \in (-\pi, \pi)$, $\theta_2 \in (-\pi, \pi)$ and $\Phi \in (-\pi, \pi)$. We will later show that under our feedback control, the value of z_1, z_2, θ_1, θ_2 and Φ remain in S if they initially belongs to S.

Our control law will be based on a candidate Lyapunov function on S as

$$V = V_1 + V_2 + \tfrac{1}{2}\, Q(\Phi), \tag{21}$$

where for $i = 1, 2$,

$$V_i = -2 \log\left(\cos \frac{\theta_i}{2}\right) + \frac{1}{2}\, h(z_i) \tag{22}$$

and $h(z)$ and $Q(\Phi)$ are smooth functions. We let $f(z) = \mathrm{d}h/\mathrm{d}z$ and $P(\Phi) = (2\pi/L)\, \mathrm{d}Q/\mathrm{d}\Phi$ and require that $h(z)$, $f(z)$, $Q(\Phi)$ and $P(\Phi)$ satisfy the following conditions:

(B1) $h(z) \to +\infty$ when $z \to c_1$ or $z \to c_2$. $Q(\Phi) \to +\infty$ when $\Phi \to \pm\pi$.
(B2) $f(z)$ and $P(\Phi)$ are monotone increasing smooth functions.
(B3) $f(c_z) = 0$ and $P(0) = 0$.

In this Lyapunov candidate function the terms V_1 and V_2 will guide the particles to follow the orbit determined by c_z. This has been shown in [29,32]. The term $Q(\Phi)$ serves as a coupling term to establish desired separation between the two particles. For example, we may let $P(\Phi) = \mathrm{atan}(\Phi/2)$ and let $Q(\Phi)$ be the integral of $P(\Phi)$.

We now design the steering control for both particles so that $\dot{V} \leqslant 0$. The derivative of the candidate Lyapunov function with respect to time is

$$\begin{aligned}
\dot{V} = {} & \frac{\sin \theta_1/2}{\cos \theta_1/2}\, \dot{\theta}_1 - \frac{1}{2}\, f(z_1) \|\nabla z_1\| \sin \theta_1 \\
& + \frac{\sin \theta_2/2}{\cos \theta_2/2}\, \dot{\theta}_2 - \frac{1}{2}\, f(z_2) \|\nabla z_2\| \sin \theta_2 \\
& + \frac{1}{2}\, P(\Phi)(\cos \theta_1 - \cos \theta_2) \\
& - \frac{1}{2}\, P(\Phi) \frac{\partial s_1}{\partial z_1} \|\nabla z_1\| \sin \theta_1 \\
& + \frac{1}{2} \frac{\partial s_2}{\partial z_2}\, P(\Phi) \|\nabla z_2\| \sin \theta_2.
\end{aligned} \tag{23}$$

We apply the identity $\cos \alpha = 1 - 2 \sin^2 \alpha/2$ so that

$$\cos \theta_1 - \cos \theta_2 = -2 \sin^2 \frac{\theta_1}{2} + 2 \sin^2 \frac{\theta_2}{2}. \tag{24}$$

We also use the fact that, for $i = 1, 2$,

$$2 \sin^2 \frac{\theta_i}{2} = \frac{\sin \theta_i/2}{\cos \theta_i/2} \sin \theta_i \quad \text{and}$$
$$\frac{1}{2} \sin \theta_i = \frac{\sin \theta_i/2}{\cos \theta_i/2} \cos^2 \frac{\theta_i}{2}. \tag{25}$$

Then, substituting the identities (24) and (25) into (23), we get

$$\begin{aligned}
\dot{V} = {} & \frac{\sin \theta_1/2}{\cos \theta_1/2} \left(\dot{\theta}_1 - f(z_1) \|\nabla z_1\| \cos^2 \frac{\theta_1}{2} - \frac{1}{2}\, P(\Phi) \sin \theta_1 \right. \\
& \left. - P(\Phi) \frac{\partial s_1}{\partial z_1} \|\nabla z_1\| \cos^2 \frac{\theta_1}{2} \right) \\
& + \frac{\sin \theta_2/2}{\cos \theta_2/2} \left(\dot{\theta}_2 - f(z_2) \|\nabla z_2\| \cos^2 \frac{\theta_2}{2} + \frac{1}{2}\, P(\Phi) \sin \theta_2 \right. \\
& \left. + P(\Phi) \frac{\partial s_2}{\partial z_2} \|\nabla z_2\| \cos^2 \frac{\theta_2}{2} \right).
\end{aligned} \tag{26}$$

We choose

$$\begin{aligned}
u_1 = {} & \kappa_{a1} \cos \theta_1 + \kappa_{b1} \sin \theta_1 \\
& - \left(f(z_1) + \frac{\partial s_1}{\partial z_1}\, P(\Phi) \right) \|\nabla z_1\| \cos^2 \frac{\theta_1}{2} \\
& - \frac{1}{2}\, P(\Phi) \sin \theta_1 + \sin \frac{\theta_1}{2},
\end{aligned}$$

$$\begin{aligned}
u_2 = {} & \kappa_{a2} \cos \theta_2 + \kappa_{b2} \sin \theta_2 \\
& - \left(f(z_2) - \frac{\partial s_2}{\partial z_2}\, P(\Phi) \right) \|\nabla z_2\| \cos^2 \frac{\theta_2}{2} \\
& + \frac{1}{2}\, P(\Phi) \sin \theta_2 + \sin \frac{\theta_2}{2},
\end{aligned} \tag{27}$$

where for $i = 1, 2$, κ_{ai} and κ_{bi} are defined in (10) but indexed by i.

Plugging (27) into (9) and (9) into (26) gives,

$$\dot{V} = -\frac{\sin^2 \theta_1/2}{\cos \theta_1/2} - \frac{\sin^2 \theta_2/2}{\cos \theta_2/2} \leqslant 0. \tag{28}$$

Note that $\dot{V}$ is finite on the state space S since $\theta_i \neq \pm\pi$.

Please cite this article as: F. Zhang, N.E. Leonard, Coordinated patterns of unit speed particles on a closed curve, Systems Control Lett. (2006), doi: 10.1016/j.sysconle.2006.10.027

The closed-loop system equations are

$$\dot{\theta}_1 = \left(f(z_1) + \frac{\partial s_1}{\partial z_1} P(\Phi) \right) \|\nabla z_1\| \cos^2 \frac{\theta_1}{2} + \frac{1}{2} P(\Phi) \sin\theta_1 - \sin\frac{\theta_1}{2},$$

$$\dot{z}_1 = -\|\nabla z_1\| \sin\theta_1,$$

$$\dot{\theta}_2 = \left(f(z_2) - \frac{\partial s_2}{\partial z_2} P(\Phi) \right) \|\nabla z_2\| \cos^2 \frac{\theta_2}{2} - \frac{1}{2} P(\Phi) \sin\theta_2 - \sin\frac{\theta_2}{2},$$

$$\dot{z}_2 = -\|\nabla z_2\| \sin\theta_2,$$

$$\dot{\Phi} = \frac{2\pi}{L} \left(\cos\theta_1 - \cos\theta_2 - \left(\frac{\partial s_1}{\partial z_1} \|\nabla z_1\| \sin\theta_1 - \frac{\partial s_2}{\partial z_2} \|\nabla z_2\| \sin\theta_2 \right) \right). \tag{29}$$

Note that the system is non-autonomous because $\partial s_1/\partial z_1$, $\partial s_2/\partial z_2$, ∇z_1 and ∇z_2 depend on time explicitly. Furthermore, $\partial s_1/\partial z_1$ and $\partial s_2/\partial z_2$ are only piecewise continuous in time.

Fortunately both the Lyapunov function and its derivative do not depend explicitly on time. We apply the invariance Theorem 4.4 on p. 192 of [14] in the following to show that as $t \to \infty$, $\theta_1 \to 0$ and $\theta_2 \to 0$.

Theorem 3. *Consider a family of orbits given by Lemmas* 1 *and* 2 *with σ being the arc-length parameter for the reference orbit with orbit value c_z. Suppose along any orbit that belongs to the set Ω in Lemma* 1, *$\partial^2 s(z,\sigma)/\partial z \partial\sigma$ is a smooth function that is not constantly zero. Suppose the initial conditions of the two particles make the initial value of V given in* (21) *finite. Then as $t \to \infty$, the states of the two particles under the control laws in* (27) *satisfy $\theta_1 \to 0$, $\theta_2 \to 0$, $z_1 \to c_z$, $z_2 \to c_z$ and $\Phi \to 0$.*

Proof. Let M be any sub-level set of V in the state space S. The value of V is finite within M. From the definition of V it is easy to see that M is compact. For $i = 1, 2$, we have

$$\frac{\partial s_i}{\partial z_i} = \int_{\sigma_{0i}}^{\sigma_i} \frac{\partial^2 s_i(z_i, \tau)}{\partial z_i \, \partial \tau} \, \mathrm{d}\tau. \tag{30}$$

By assumption, the integrand $\partial^2 s_i(z_i,\tau)/\partial z_i \partial\tau$ is a smooth function on the compact sub-level set M and hence is bounded both below and above. Since $\sigma_i - \sigma_{0i} \in [0, L)$, we know that $|\partial s_i/\partial z_i|$ is bounded. We also know that $\|\nabla z_i\|$ is bounded for all the possible orbits. Therefore, the right-hand side of the closed-loop system given by (29) satisfies the Lipschitz condition on M. As guaranteed by the derivative of the Lyapunov function V being non-positive, starting within the set M, a solution will not escape M. Therefore, starting from any point in M, the solution of the closed-loop system exists and is unique for $t \in [0, \infty)$.

The finiteness of the initial value of V guarantees that initially $z_i \neq c_1$ and $z_i \neq c_2$ on the state space S where V is defined. Therefore, initially $z_i \in (c_1, c_2)$. Since V never increases, the particles will stay in Ω given in Lemma 1. As $t \to \infty$, using Theorem 4.4 in [14], we can conclude that $\sin\theta_1/2$ and $\sin\theta_2/2$ vanish. In this case, since the initial value of V is finite and V is not increasing, then starting in the interval $(-\pi, \pi)$, θ_1 and θ_2 can only converge to zero. This means that the controlled dynamics converge to a subset E of the state space with $\theta_1 = \theta_2 = 0$. According to the closed-loop system equations in (29), this also implies that $\dot{z}_i \to 0$ and $\dot{\Phi} \to 0$ on the set E.

We next prove that $\dot{\theta}_1 \to 0$ and $\dot{\theta}_2 \to 0$ by the following steps:

(S1) Note that $\dot{\theta}_1$ and $\dot{\theta}_2$ are piecewise continuous functions of time t.

(S2) In the set E where z_1, z_2 and Φ are constant, the functions $(f(z_1) + (\partial s_1/\partial z_1) P(\Phi))\|\nabla z_1\|$ and $(f(z_2) - (\partial s_2/\partial z_2 P(\Phi))\|\nabla z_2\|$ are piecewise uniformly continuous functions of t when the particles move along the orbits determined by z_1 and z_2. *Proof for* (S2): Since z_1, z_2 and Φ are constant and $\|\nabla z_i\|$ are smooth functions with bounded derivatives in the set E, we only need to show that $\partial s_i/\partial z_i$ are piecewise uniformly continuous functions of t for $i = 1, 2$. Because z_i is constant,

$$\frac{\mathrm{d}}{\mathrm{d}t} \frac{\partial s_i}{\partial z_i} = \frac{\partial^2 s_i(z_i, s_i)}{\partial z_i \, \partial s_i} \frac{\mathrm{d}s_i}{\mathrm{d}t}. \tag{31}$$

We know $\partial s_i(z_i, s_i)/\partial z_i \partial s_i$ is bounded in the set E and

$$\left| \frac{\mathrm{d}s_i}{\mathrm{d}t} \right| = \left| \cos\theta_i - \frac{\partial s_i}{\partial z_i} \|\nabla z_i\| \sin\theta_i \right| = 1 \tag{32}$$

because $\theta_i = 0$. Therefore, $\partial s_i/\partial z_i$ has bounded derivative with respect to t. Furthermore, because z_i is constant, discontinuity in $\partial s_i/\partial z_i$ only happens when the curve length s_i between the particle and the starting point changes from L to 0. The interval between two consecutive discontinuities in $\partial s_i/\partial z_i$ has length L. Applying Corollary 7 in the Appendix, we have shown that $\partial s_i/\partial z_i$ are piecewise uniformly continuous for $i = 1, 2$. Next, applying Corollary 8 in the Appendix, we conclude $(f(z_1) + (\partial s_1/\partial z_1) P(\Phi))\|\nabla z_1\|$ and $(f(z_2) - (\partial s_2/\partial z_2) P(\Phi))\|\nabla z_2\|$ are piecewise uniformly continuous functions of time in the set E.

(S3) Since $\theta_i(t) \to 0$ for $i = 1, 2$, $\dot{\theta}_1(t) \to (f(z_1) + (\partial s_1/\partial z_1) P(\Phi))\|\nabla z_1\|$ and $\dot{\theta}_2(t) \to (f(z_2) - (\partial s_2/\partial z_2) P(\Phi))\|\nabla z_2\|$ in the set E where z_1, z_2 and Φ are constant, Lemma 9 in the Appendix leads us to the conclusion that $\dot{\theta}_i \to 0$ for $i = 1, 2$.

The fact that $\dot{\theta}_1(t) \to 0$ and $\dot{\theta}_2(t) \to 0$ when $t \to \infty$ implies that

$$\left(f(z_1) + \frac{\partial s_1}{\partial z_1} P(\Phi) \right) \|\nabla z_1\| \to 0$$

and

$$\left(f(z_2) - \frac{\partial s_2}{\partial z_2} P(\Phi) \right) \|\nabla z_2\| \to 0 \tag{33}$$

as $t \to \infty$. The finiteness of the initial value of V guarantees that the particles will stay in Ω. Thus $\|\nabla z_1\|$ and $\|\nabla z_2\|$ cannot be zero. Therefore $f(z_1) + (\partial s_1/\partial z_1)P(\Phi) \to 0$ and $f(z_2) - (\partial s_2/\partial z_2)P(\Phi) \to 0$ as $t \to \infty$.

We know that $\partial s_1/\partial z_1$ and $\partial s_2/\partial z_2$ are time varying on the set E. Then because $f(z_1)$, $f(z_2)$ and $P(\Phi)$ are constants we can conclude that they all vanish. This implies that $z_1 \to c_z$, $z_2 \to c_z$ and $\Phi \to 0$. $\square$

5. Pattern for N particles

The control law (27) can be generalized to stabilize patterns involving N particles moving along a single-looped regular curve. For $N > 2$, the coupling schemes for the ψ_i, $i = 1, 2, \ldots, N$, are not unique. We consider the "chain" case, where except for particle N, each particle is coupled to the next particle according to given indices. We define, for $j = 1, 2, \ldots, N-1$, $\Phi_j = \psi_j - \psi_{j+1} - 2\pi c_s^j/L$ where c_s^j is the desired separation between particles j and $j+1$. We then define functions $Q_j(\Phi_j)$ and $P_j(\Phi_j)$ so that $P_j = (2\pi/L)\mathrm{d}Q_j/\mathrm{d}\Phi_j$ and the following properties are satisfied for $j = 1, 2, \ldots, N-1$:

(C1) $Q_j(\Phi_j) \to +\infty$ as $\Phi_j \to \pm\pi$,
(C2) $P_j(\Phi_j)$ is a monotone increasing function,
(C3) $P_j(0) = 0$.

We define $V_i = -2\log(\cos\theta_i/2) + \frac{1}{2}h(z_i)$ for $i = 1, 2, \ldots, N$. The derivative of V_i along the controlled dynamics is

$$\dot{V}_i = \frac{\sin\theta_i/2}{\cos\theta_i/2}\dot{\theta}_i - \frac{1}{2}f(z_i)\|\nabla z_i\|\sin\theta_i. \tag{34}$$

For the N particle pattern, the total Lyapunov function is

$$V_L = \sum_{i=1}^{N} V_i + \frac{1}{2}\sum_{j=1}^{N-1} Q_j(\Phi_j). \tag{35}$$

The derivative of $Q_j(\Phi_j)$ is

$$\begin{aligned}
\dot{Q}_j(\Phi_j) &= \frac{1}{2}P_j(\Phi_j)(\cos\theta_j - \cos\theta_{j+1}) \\
&\quad - \frac{1}{2}P_j(\Phi_j)\frac{\partial s_j}{\partial z_j}\|\nabla z_j\|\sin\theta_j \\
&\quad + \frac{1}{2}\frac{\partial s_{j+1}}{\partial z_{j+1}}P_j(\Phi_j)\|\nabla z_{j+1}\|\sin\theta_{j+1} \\
&= -P_j(\Phi_j)\sin^2\frac{\theta_j}{2} - \frac{1}{2}P_j(\Phi_j)\frac{\partial s_j}{\partial z_j}\|\nabla z_j\|\sin\theta_j \\
&\quad + P_j(\Phi_j)\sin^2\frac{\theta_{j+1}}{2} + \frac{1}{2}\frac{\partial s_{j+1}}{\partial z_{j+1}} \\
&\quad \times P_j(\Phi_j)\|\nabla z_{j+1}\|\sin\theta_{j+1}.
\end{aligned} \tag{36}$$

For convenience we define $\Phi_0 = \Phi_N \equiv 0$ and $P_0(\Phi_0) = P_N(\Phi_N) \equiv 0$. $P_0(\Phi_0)$ and $P_N(\Phi_N)$ will be used purely as place holders in computing the derivative of the Lyapunov function along the controlled dynamics. We compute

$$\begin{aligned}
\dot{V}_L &= \sum_{i=1}^{N}\dot{V}_i + \frac{1}{2}\sum_{j=1}^{N-1}\dot{Q}_j(\Phi_j) \\
&= \sum_{j=1}^{N}\left(\frac{\sin\theta_j/2}{\cos\theta_j/2}\left(\dot{\theta}_j - f(z_j)\|\nabla z_j\|\cos^2\frac{\theta_j}{2}\right.\right. \\
&\quad - \frac{1}{2}(P_j(\Phi_j) - P_{j-1}(\Phi_{j-1}))\sin\theta_j \\
&\quad \left.\left. -(P_j(\Phi_j) - P_{j-1}(\Phi_{j-1}))\frac{\partial s_j}{\partial z_j}\|\nabla z_j\|\cos^2\frac{\theta_j}{2}\right)\right).
\end{aligned} \tag{37}$$

We now design the control law to be

$$\begin{aligned}
u_j &= \kappa_{aj}\cos\theta_j + \kappa_{bj}\sin\theta_j \\
&\quad - \left(f(z_j) + \frac{\partial s_j}{\partial z_j}(P_j(\Phi_j) - P_{j-1}(\Phi_{j-1}))\right) \\
&\quad \times \|\nabla z_j\|\cos^2\frac{\theta_j}{2} \\
&\quad - \frac{1}{2}(P_j(\Phi_j) - P_{j-1}(\Phi_{j-1}))\sin\theta_j + \sin\frac{\theta_j}{2}
\end{aligned} \tag{38}$$

for $j = 1, 2, \ldots, N$ where κ_{aj} and κ_{bj} are defined in (10) but indexed by j. This will result in

$$\dot{V}_L = -\sum_{j=1}^{N}\frac{\sin^2\theta_j/2}{\cos\theta_j/2} \leqslant 0. \tag{39}$$

The closed-loop system equations are

$$\begin{aligned}
\dot{\theta}_i &= \left(f(z_i) + \frac{\partial s_i}{\partial z_i}(P_i(\Phi_i) - P_{i-1}(\Phi_{i-1}))\right)\|\nabla z_i\|\cos^2\frac{\theta_i}{2} \\
&\quad + \frac{1}{2}(P_i(\Phi_i) - P_{i-1}(\Phi_{i-1}))\sin\theta_i - \sin\frac{\theta_i}{2}, \\
\dot{\Phi}_j &= \frac{2\pi}{L}\left(\cos\theta_j - \cos\theta_{j+1} - \left(\frac{\partial s_j}{\partial z_j}\|\nabla z_j\|\sin\theta_j\right.\right. \\
&\quad \left.\left. - \frac{\partial s_{j+1}}{\partial z_{j+1}}\|\nabla z_{j+1}\|\sin\theta_{j+1}\right)\right), \\
\dot{z}_i &= -\|\nabla z_i\|\sin\theta_i,
\end{aligned} \tag{40}$$

where $i = 1, 2, \ldots, N$ and $j = 1, 2, \ldots, N-1$.

Corollary 4. *Consider a family of orbits given by Lemmas 1 and 2 with σ being the arc-length parameter for the reference orbit with orbit value c_z. Suppose along any orbit that belongs to the set Ω in Lemma 1, $\partial^2 s(z,\sigma)/\partial z\partial\sigma$ is a smooth function that is not constantly zero. Suppose the initial conditions of the N particles make the initial value of V_L given in (35) finite. Then under the control law given by (38), as $t \to \infty$, the states of the particles satisfy $\theta_i \to 0$ and $z_i \to c_z$ for $i = 1, 2, \ldots, N$ and $\Phi_j \to 0$ for $j = 1, 2, \ldots, N-1$.*

Proof. As in the proof of Theorem 3, we conclude that as $t \to \infty$, $\theta_i \to 0$ for all $i = 1, 2, \ldots, N$. We define a subset E of the state space where all θ_i vanish, z_i are constant and Φ_j are

Please cite this article as: F. Zhang, N.E. Leonard, Coordinated patterns of unit speed particles on a closed curve, Systems Control Lett. (2006), doi: 10.1016/j.sysconle.2006.10.027

constant for $i = 1, 2, \ldots, N$ and $j = 1, 2, \ldots, N-1$. On this subset E, the closed-loop system equations for $\dot{\theta}_i$ are

$$\dot{\theta}_i = \left(f(z_i) + \frac{\partial s_i}{\partial z_i}(P_i(\Phi_i) - P_{i-1}(\Phi_{i-1})) \right) \|\nabla z_i\|, \tag{41}$$

where $i = 1, 2, \ldots, N$. We can show that the right-hand side of (41) is uniformly piecewise continuous. We then apply Lemma 9 in the Appendix to claim that $\dot{\theta}_i \to 0$ which further implies that $f(z_i) + (\partial s_i/\partial z_i)(P_i(\Phi_i) - P_{i-1}(\Phi_{i-1})) \to 0$ for $i = 1, 2, \ldots, N$. Because $\partial s_i/\partial z_i$ is time varying but $f(z_i)$ and $P_i(\Phi_i)$ are constant on the set E, then $f(z_i) \to 0$ and $P_i(\Phi_i) - P_{i-1}(\Phi_{i-1}) \to 0$ for all $i = 0, 1, \ldots, N$. Since $P_0(\Phi_0) = P_N(\Phi_N) = 0$, we conclude that $P_i(\Phi_i) \to 0$ for $i = 1, 2, \ldots, N-1$. □

6. Simulation results

We first show one example of stabilizing an invariant pattern for two particles moving on the super-ellipse given by $x^{2p}/a_0^{2p} + y^{2p}/b_0^{2p} = 1$ where $a_0 > 0$ and $b_0 > 0$. Notice that when $p = 1$ this describes an ellipse. When p is an odd integer greater than one, the curve looks like a rectangle with rounded corners. We construct the orbit function $z(x, y) = (x^{2p} + y^{2p}/e^{2p})^{1/2p}$ where $e = b_0/a_0$. If p is an odd integer, the curve with orbit value a_0 can be parametrized by $x = a_0(\cos\theta)^{1/p}$ and $y = b_0(\sin\theta)^{1/p}$. From these equations, we are able to compute the arc-length, curvature and tangent vectors of any super-ellipse in the family. For coupling between two particles, we let $P(\Phi) = K\,\mathrm{atan}(\Phi/2)$ where the gain $K > 0$ can be adjusted for performance.

In our simulation, we first control the two unit speed particles so that they move to the outer super-ellipse shown in Fig. 3 with $a_0 = 4$, $b_0 = 3$, $p = 3$ and relative arc-length equal to 2. Then we command them to the inner super-ellipse with $a_0 = 3$, $b_0 = 2$, $p = 3$ and relative arc-length equal to 1. Fig. 3 shows the trajectories and Fig. 4 shows the arc-length separation with respect to time. Notice that we do not change the control law, we only change the value of the parameters a_0 and b_0 for the transition to happen.

In Fig. 5, we demonstrate the control of eight particles to invariant patterns along various star shapes that can be constructed using the formula in [28]. We control the particles to distribute uniformly on each star. The communication topology is a chain i.e., the jth particle is coupled to the $(j-1)$th and $(j+1)$th particle for $j = 2, 3, \ldots, N-1$; the first and last particles are only coupled to one other particle and not to each other.

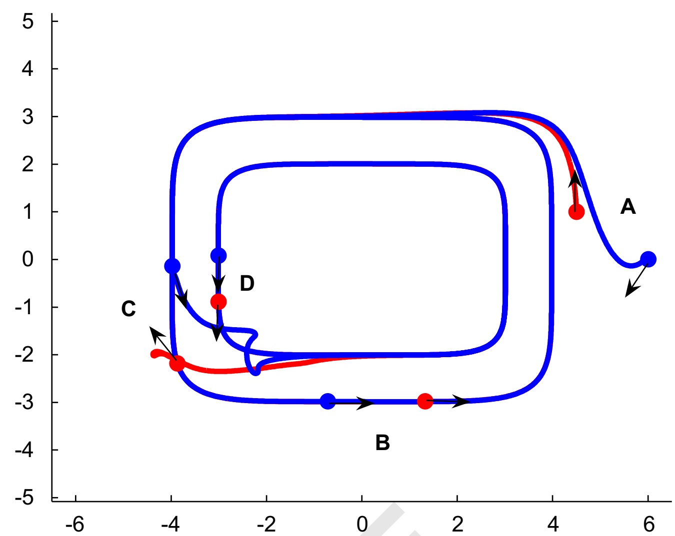

Fig. 3. The trajectories of two unit speed particles stabilized to invariant patterns on super-ellipses. The outer super-ellipse has $a_0 = 4$, $b_0 = 3$ and $p = 3$ and the inner super-ellipse has $a_0 = 3$, $b_0 = 2$ and $p = 3$. The desired relative separation, measured by the arc-length difference, is 2 on the outer super-ellipse and 1 on the inner super-ellipse. Label A indicates the initial positions of the two particles. Label B indicates the stabilized pattern on the outer super-ellipse. Label C indicates when the two particles start to move from the outer super-ellipse to the inner super-ellipse. Label D indicates the stabilized pattern on the inner super-ellipse.

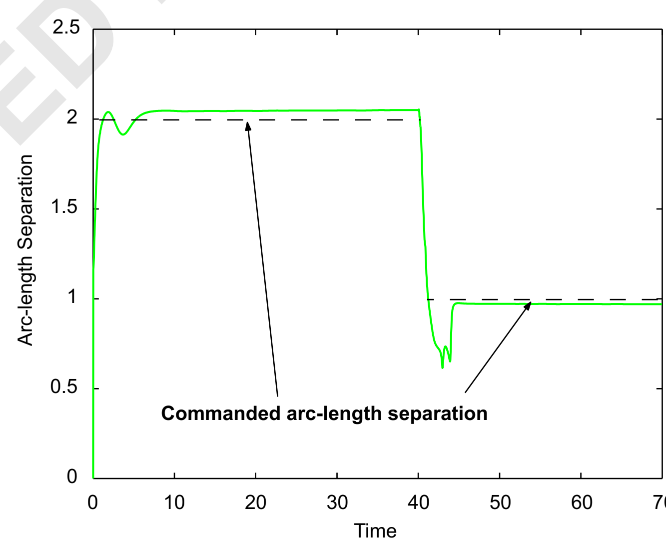

Fig. 4. The arc-length difference between the two unit speed particles versus time for stabilization of two particles moving around super-ellipses.

7. Summary and future directions

In this paper, we have introduced a new method for designing steering control laws for a system of N unit speed particles. The control steers the particles to an invariant pattern corresponding to a constant orbit value and constant separations measured by the relative arc-lengths along the reference orbit. By extending curve tracking methods, we prove convergence to closed simple smooth curves. This class of curves is much more general than what were treated in recent related works (e.g. [11,24]). Although the convergence is not global in the plane, the orbit function we introduce often allows convergence from a large set of initial positions.

In our cooperative control laws, we use relative arc-length to couple particles because of the constant speed constraint. A simple chain structure for coupling allows us to stabilize the invariant patterns. Other more complicated coupling structures may also be applied according to communication or sensing

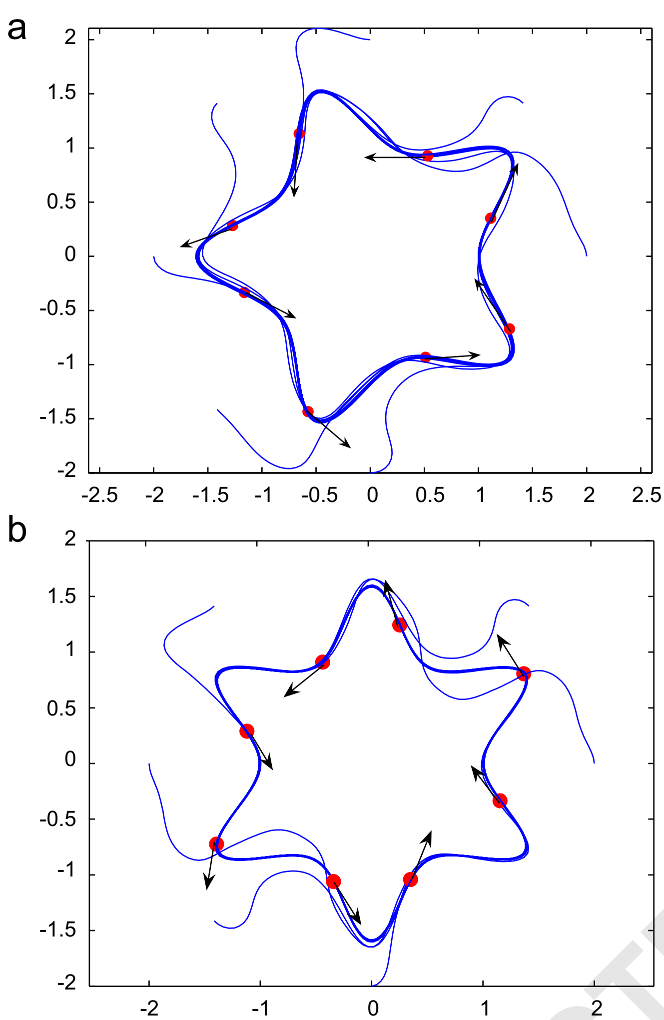

Fig. 5. Patterns of eight unit speed particles on two star-shaped curves. The particles are distributed uniformly as they move around each curve: (a) five point star and (b) six point star.

requirements. We have not yet addressed collision avoidance in this setting. The challenge here derives from the constant speed constraint. In practice, extra collision avoidance mechanisms are often introduced that break the constant speed constraint when safety instead of performance is the major concern.

The problem of stabilizing an invariant pattern along or near a closed curve or boundary is also interesting if the constant speed constraint is relaxed. In [3], a PDE-based algorithm inspired by computer vision algorithms [13] is developed to distribute agents along a boundary. Convergence is demonstrated but not yet proved. In recent preprint [7], Kumar and Hsieh have shown some interesting theoretical and simulation results using potential functions. Some experimental works are documented in [5]. Our results, although based on the assumption that all particles travel at identical constant speed, suggest a systematic approach to solving this pattern generation problem. We have shown some of our results on achieving invariant patterns without the constant speed constraint in [36].

This paper is concerned with the planar setting. Of course, many important motion control problems evolve in three-dimensional physical space. For underwater gliders, our results are applied by projecting the three-dimensional motion onto the plane [30]. New developments have been made in [12] to use a natural frame setting to model three-dimensional motion. The resulting steering laws are similar to those derived in the planar setting. This suggests that the concepts of orbit function and relative arc-length coupling established in this paper can also be extended to the three-dimensional setting.

Acknowledgments

The authors would like to thank Derek Paley for collaborations and discussions. This work was supported in part by ONR Grants N00014–02–1–0826 and N00014–04–1–0534.

Appendix A. Uniformly continuous functions

We first review one classical result on uniformly continuous functions cf. [23,26].

Theorem 5. *Suppose $\phi(t)$ is differentiable on $[0, \infty)$ and $|\phi'|$ is bounded. Then $\phi(t)$ is uniformly continuous.*

The concept of uniformly continuous can be extended to piecewise continuous functions.

Definition 6. A piecewise continuous function is piecewise uniformly continuous on $[t_0, \infty)$ if $\forall k_1 > 0$ and $\forall T_1 > t_0$, $\exists k_2$ such that either $\forall t \in [T_1, T_1 + k_2)$, $|\phi(t) - \phi(T_1)| < \frac{1}{2}k_1$ or alternatively, $\forall t \in (T_1 - k_2, T_1]$, $|\phi(t) - \phi(T_1)| < \frac{1}{2}k_1$.

We have the following corollaries for piecewise uniform continuity.

Corollary 7. *Suppose a piecewise continuous function $\phi(t)$ is differentiable on $[t_0, \infty)$ except for the points where discontinuities occur. Suppose $|\phi'|$, when it exists, is bounded by $N_b > 0$. Suppose the length of each sub-interval where $\phi(t)$ is differentiable is bounded below by $l > 0$. Then $\phi(t)$ is piecewise uniformly continuous.*

Corollary 8. *Let $\phi_1(t)$ be uniformly continuous and $\phi_2(t)$ be piecewise uniformly continuous on $[t_0, \infty)$, then*

(1) *$(\phi_1(t) + \phi_2(t))$ is piecewise uniformly continuous on $[t_0, \infty)$;*
(2) *$\phi_3(\phi_2(t))$ is piecewise uniformly continuous if ϕ_3 is a smooth function on the image of $\phi_2(t)$ and $|\phi_3'|$ is bounded;*
(3) *$\phi_1(t)\phi_2(t)$ is piecewise uniformly continuous if $|\phi_1(t)|$ and $|\phi_2(t)|$ are bounded.*

The well-known Barbalat's lemma can be generalized to piecewise uniformly continuous functions.

Lemma 9. *Let ϕ be a piecewise continuous function and η be a piecewise uniformly continuous function on $[t_0, \infty)$. Sup-*

Please cite this article as: F. Zhang, N.E. Leonard, Coordinated patterns of unit speed particles on a closed curve, Systems Control Lett. (2006), doi: 10.1016/j.sysconle.2006.10.027

pose that $\lim_{t\to\infty}\int_{t_0}^{t}\phi(\sigma)\,\mathrm{d}\sigma$ *exists and is finite. Suppose that* $\lim_{t\to\infty}(\phi(t)-\eta(t))=0$. *Then* $\phi(t)\to 0$ *as* $t\to\infty$.

Proof. If $\phi(t)$ does not go to zero, then $\eta(t)$ does not go to zero either. Since $\eta(t)$ does not go to zero, there exists positive k_1 such that for every $T>t_0$, we can find T_1 and k where $T_1\geqslant T+k$ so that $|\eta(T_1)|\geqslant k_1$. By the assumption that $\eta(t)$ is piecewise uniformly continuous, given k_1, T_1 and k, there exists positive $k_2<k$ such that $|\eta(t)-\eta(T_1)|<k_1/2$ either for all $t\in[T_1,T_1+k_2]$ or for all $t\in[T_1-k_2,T_1]$.

Hence either for all $t\in[T_1,T_1+k_2]$ or for all $t\in[T_1-k_2,T_1]$, we must have

$$\begin{aligned}|\eta(t)| &= |\eta(t)-\eta(T_1)+\eta(T_1)|\\ &\geqslant |\eta(T_1)|-|\eta(t)-\eta(T_1)|>k_1-\tfrac{1}{2}k_1=\tfrac{1}{2}k_1.\end{aligned}\tag{A.1}$$

Therefore, either

$$\left|\int_{T_1}^{T_1+k_2}\eta(t)\,\mathrm{d}t\right|=\int_{T_1}^{T_1+k_2}|\eta(t)|\,\mathrm{d}t>\frac{1}{2}k_1k_2\tag{A.2}$$

or

$$\left|\int_{T_1-k_2}^{T_1}\eta(t)\,\mathrm{d}t\right|=\int_{T_1-k_2}^{T_1}|\eta(t)|\,\mathrm{d}t>\frac{1}{2}k_1k_2\tag{A.3}$$

is true. The equality holds since $\eta(t)$ retains the same sign for $t\in[T_1,T_1+k_2)$ or for $t\in(T_1-k_2,T_1]$.

We define a function $\xi(t)=\phi(t)-\eta(t)$. Since $\xi(t)\to 0$ as $t\to\infty$, then for the positive number $k_1/4$, we can find a time $T^*>0$ such that $|\xi(t)|<k_1/4$ for all $t>T^*$. Then for any $T>T^*$, we let $T_1\geqslant T+k_2$ so that one of (A.2) and (A.3) is satisfied. For $t\in[T_1-k_2,T_1]$ and $t\in[T_1,T_1+k_2]$, we still have $|\xi(t)|<k_1/4$. Therefore, either

$$\left|\int_{T_1}^{T_1+k_2}\xi(t)\,\mathrm{d}t\right|\leqslant\int_{T_1}^{T_1+k_2}|\xi(t)|\,\mathrm{d}t<\frac{1}{4}k_1k_2\tag{A.4}$$

or

$$\left|\int_{T_1-k_2}^{T_1}\xi(t)\,\mathrm{d}t\right|\leqslant\int_{T_1-k_2}^{T_1}|\xi(t)|\,\mathrm{d}t<\frac{1}{4}k_1k_2\tag{A.5}$$

is true. We then have either

$$\begin{aligned}\left|\int_{T_1}^{T_1+k_2}\phi(t)\,\mathrm{d}t\right| &= \left|\int_{T_1}^{T_1+k_2}(\eta(t)+\xi(t))\,\mathrm{d}t\right|\\ &\geqslant \left|\int_{T_1}^{T_1+k_2}\eta(t)\,\mathrm{d}t\right|-\left|\int_{T_1}^{T_1+k_2}\xi(t)\,\mathrm{d}t\right|\\ &> \frac{1}{4}k_1k_2\end{aligned}\tag{A.6}$$

or

$$\begin{aligned}\left|\int_{T_1-k_2}^{T_1}\phi(t)\,\mathrm{d}t\right| &= \left|\int_{T_1-k_2}^{T_1}(\eta(t)+\xi(t))\,\mathrm{d}t\right|\\ &\geqslant \left|\int_{T_1-k_2}^{T_1}\eta(t)\,\mathrm{d}t\right|-\left|\int_{T_1-k_2}^{T_1}\xi(t)\,\mathrm{d}t\right|\\ &> \frac{1}{4}k_1k_2.\end{aligned}\tag{A.7}$$

In summary, we have shown that there exists a time $T^*>t_0$ such that for any $T>T^*$, there exists $k_2>0$ and $T_1>T+k_2$ such that one of (A.6) and (A.7) is satisfied. Thus the integral $\int_{t_0}^{t}\phi(\sigma)\,\mathrm{d}\sigma$ cannot converge to a finite limit as $t\to\infty$, a contradiction. This proof is inspired by a proof for an extension of Barbalat's lemma in [17]. □

References

[1] Adaptive Sampling and Prediction (ASAP) Project, URL: ⟨http://www.princeton.edu/~dcsl/asap/ ⟩.
[2] C. Belta, V. Kumar, Abstraction and control for groups of robots, IEEE Trans. Robot. 20 (5) (2004) 865–875.
[3] A.L. Bertozzi, M. Kemp, D. Marthaler, Determining environmental boundaries: asynchronous communication and physical scales, in: V. Kumar, N. Leonard, A. Morse (Eds.), Cooperative Control, A Post-Workshop Volume: 2003 Block Island Workshop on Cooperative Control, Springer, Berlin, 2005, pp. 35–42.
[4] A.M. Bloch, D.E. Chang, N.E. Leonard, J.E. Marsden, Controlled Lagrangians and the stabilization of mechanical systems II: potential shaping, IEEE Trans. Automat. Control 46 (10) (2001) 1556–1571.
[5] J. Clark, R. Fierro, Cooperative hybrid control of robotic sensors for perimeter detection and tracking, in: Proceedings of American Control Conference, Portland, OR, 2006, pp. 3500–3505.
[6] D. Culler, D. Estrin, M. Srivastava, Overview of sensor networks, IEEE Comput. Mag. 37 (8) (2004) 41–49.
[7] M.A. Hsieh, V. Kumar, Pattern generation with multiple robots, in: IEEE International Conference on Robotics and Automation, Orlando, FL, 2006, pp. 2442–2447.
[8] A. Jadbabaie, J. Lin, A.S. Morse, Coordination of groups of mobile agents using nearest neighbor rules, IEEE Trans. Automat. Control 48 (6) (2003) 988–1001.
[9] E.W. Justh, P.S. Krishnaprasad, A simple control law for UAV formation flying, ISR Technical Report, TR2002-38, 2002.
[10] E.W. Justh, P.S. Krishnaprasad, Steering laws and continuum models for planar formations, in: Proceedings of 42nd IEEE Conference on Decision and Control, Maui, Hawaii, 2003, pp. 3609–3614.
[11] E.W. Justh, P.S. Krishnaprasad, Equilibria and steering laws for planar formations, Syst. Control Lett. 52 (1) (2004) 25–38.
[12] E.W. Justh, P.S. Krishnaprasad, Natural frames and interacting particles in three dimensions, in: Proceedings of 44th IEEE Conference on Decision and Control, Seville, Spain, 2005, pp. 2841–2846.
[13] M. Kass, A. Witkin, D. Terzopolous, Snakes: active contour models, Int. J. Comput. Vision 1 (1987) 321–331.
[14] H. Khalil, Nonlinear Systems, second ed., Prentice-Hall, Englewood Cliffs, NJ, 1995.
[15] N.E. Leonard, D. Paley, F. Lekien, R. Sepulchre, D. Fratantoni, R. Davis, Collective motion, sensor networks and ocean sampling, Proc. IEEE, 2007, to appear.
[16] S. Martínez, F. Bullo, Optimal sensor placement and motion coordination for target tracking, Automatica 42 (4) (2006) 661–668.
[17] A. Micaelli, C. Samson, Trajectory tracking for unicycle-type and two-steering-wheels mobile robots, INRIA Report, 2097, 1993.
[18] R.S. Millman, G.D. Parker, Elements of Differential Geometry, Prentice-Hall, Englewood Cliffs, NJ, 1977.
[19] P. Ogren, E. Fiorelli, N.E. Leonard, Formations with a mission: stable coordination of vehicle group maneuvers, in: Proceedings of 15th International Symposium on Mathematical Theory of Networks and Systems, 2002.
[20] P. Ogren, E. Fiorelli, N.E. Leonard, Cooperative control of mobile sensor networks: adaptive gradient climbing in a distributed environment, IEEE Trans. Automat. Control 49 (8) (2004) 1292–1302.
[21] R. Olfati-Saber, R.M. Murray, Consensus problems in networks of agents with switching topology and time-delays, IEEE Trans. Automat. Control 49 (9) (2004) 1520–1533.
[22] J. Parrish, W. Hamner (Eds.), Animal Groups in Three Dimensions, Cambridge University Press, Cambridge, 1997.

Please cite this article as: F. Zhang, N.E. Leonard, Coordinated patterns of unit speed particles on a closed curve, Systems Control Lett. (2006), doi: 10.1016/j.sysconle.2006.10.027

[23] R.T. Seeley, Calculus of One Variable, Scott, Foresman and Company, 1968 pp. 472–474.
[24] R. Sepulchre, D. Paley, N.E. Leonard, Stabilization of planar collective motion: all-to-all communication, IEEE Transactions on Automatic Control, to appear.
[25] S. Strogatz, From Kuramoto to Crawford: exploring the onset of synchronization in populations in coupled oscillators, Physica D 143 (2000) 1–20.
[26] D. Sweet, Lecture Notes for Advanced Calculus, Department of Mathematics, University of Maryland, College Park, MD, 1999.
[27] L.-S. Wang, P.S. Krishnaprasad, Gyroscopic control and stabilization, J. Nonlinear Sci. 2 (1992) 367–415.
[28] E.W. Weisstein, "superellipse", From MathWorld—A Wolfram Web Resource, URL: ⟨http://mathworld.wolfram.com/Superellipse.html⟩.
[29] F. Zhang, Geometric cooperative control of formations, Ph.D. Thesis, University of Maryland, 2004.
[30] F. Zhang, D.M. Fratantoni, D. Paley, J. Lund, N.E. Leonard, Control of coordinated patterns for ocean sampling, preprint, 2006.
[31] F. Zhang, M. Goldgeier, P.S. Krishnaprasad, Control of small formations using shape coordinates, in: Proceedings of International Conference of Robotics and Automation, Taipei, Taiwan, 2003, pp. 2510–2515.
[32] F. Zhang, E. Justh, P.S. Krishnaprasad, Boundary following using gyroscopic control, in: Proceedings of 43rd IEEE Conference on Decision and Control, Atlantis, Paradise Island, Bahamas, 2004, pp. 5204–5209.
[33] F. Zhang, P.S. Krishnaprasad, Formation dynamics under a class of control laws, in: Proceedings of American Control Conference, Anchorage, AK, 2002, pp. 1678–1685.
[34] F. Zhang, P.S. Krishnaprasad, Co-ordinated orbit transfer of satellite clusters, astrodynamics, space missions, and chaos, Ann. New York Acad. Sci. 1017 (2004) 112–137.
[35] F. Zhang, N. Leonard, Generating contour plots using multiple sensor platforms, in: Proceedings of IEEE Symposium on Swarm Intelligence, Pasadena, CA, 2005, pp. 309–314.
[36] F. Zhang, N. Leonard, Coordinated patterns on smooth curves, in: Proceedings of IEEE International Conference on Networking, Sensing and Control, Ft. Lauderdale, FL, 2006, pp. 434–440.

Please cite this article as: F. Zhang, N.E. Leonard, Coordinated patterns of unit speed particles on a closed curve, Systems Control Lett. (2006), doi: 10.1016/j.sysconle.2006.10.027